Metallomics

Accepted Manuscript

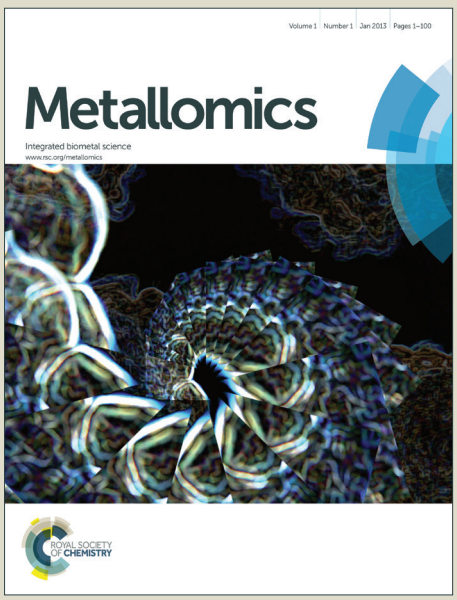

ROYAL SOCIETY OF CHEMISTRY

www.rsc.org/metallomics

Table of Contents Entry, MT-ART-07-2014-000196

Disruption of possible endocytic recycling pathways disturbs cellular copper and zinc accumulation in *Drosophila*

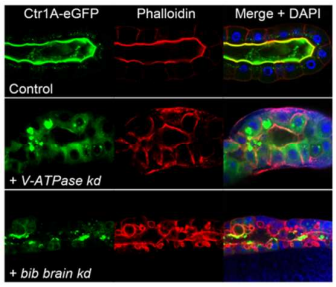

Title:

Vacuolar-type H^+-ATPase subunits and the neurogenic protein big brain are required for optimal copper and zinc uptake

Authors:

Jianbin Wang, Tim Binks, Coral G Warr and Richard Burke

Affiliations:

School of Biological Sciences, Monash University, Melbourne, Victoria, Australia

ABSTRACT

Copper and zinc homeostasis in polarized epithelial cells requires the correct localization and regulation of membrane-bound transport proteins at the apical and basolateral cell membranes. We have identified a subunit of the vacuolar-type H^+-ATPase (V-ATPase) complex, vhaPPA1-2, and the *Drosophila* aquaporin homolog big brain (bib), as being required for the correct localization of the copper uptake transporters Ctr1A and Ctr1B and the zinc uptake protein dZip89B and hence necessary for optimal copper and zinc accumulation *in vivo*. Knockdown of *vhaPPA1-2* or *bib* resulted in cuticle hypo-pigmentation phenotypes typical of copper deficiency in the fly and induction of midgut *Ctr1B* expression, a known response to low cellular copper levels. Furthermore, midgut-specific knockdown of *bib* increased tolerance to elevated dietary zinc levels. Ctr1A, Ctr1B and dZip89B are normally localized to the apical plasma membrane. Upon knockdown of *vhaPPA1-2* or *bib*, this localization was strongly disrupted as was that of the generic plasma membrane marker CD8-GFP, indicating that these two genes are not acting specifically on metal ion homeostasis but rather are necessary for general apical membrane protein localization in polarized epithelial cells. These results suggest that metal ion transport is particularly sensitive to disturbances in cellular protein localization processes.

Keywords:

Drosophila; copper homeostasis; Vacuolar-type H^+-ATPase; big brain; zinc homeostasis

INTRODUCTION

Regulated copper and zinc uptake is needed in numerous eukaryotic cell types to supply the metal ions needed for the activity of essential cuproenzymes including superoxide dismutase and cytochrome C oxidase [1] and numerous zinc-dependent proteins [2] such as the zinc-finger transcription factors [3] and enzymes like alkaline phosphatase and the matrix metalloproteinases [4, 5]. Copper and zinc are highly toxic too and metal overload in cells must be avoided either through sequestration by metallothionein proteins [6, 7] or by balancing uptake and efflux to maintain safe intracellular levels.

Copper uptake is chiefly mediated by members of the Ctr family of transmembrane domain proteins [8], which form trimeric pores allowing the regulated transport of copper across the membrane [9, 10]. Ctr1 is the main vertebrate uptake transporter and is normally located on the apical plasma membrane (PM) of numerous tissues [11]. Post-translational regulation of hCtr1 has been reported, with copper-induced endocytosis thought to restrict copper uptake in high-copper environments [12] although others have not been able to detect such regulation [13, 14]. Copper efflux is mediated by members of the P-type ATPase family, ATP7A and B, which are normally found at the *trans*-Golgi network (TGN) membrane, where they supply copper to secretory pathway proteins such as tyrosinase and ceruloplasmin [15]. Under high cellular copper conditions, these transporters can translocate to the outer PM or to vesicles just adjacent to the outer membrane [16] in order to facilitate copper efflux.

Transport of zinc across cell membranes is mediated by Zip and ZnT proteins [17, 18]. The Zip (Zrt / IRT-like / SLC39A) transmembrane-domain proteins transport zinc into the cytosol, either from outside the cell or releasing it from the lumen of organelles such as the endoplasmic reticulum, TGN and storage vesicles. Conversely, members of the ZnT (cation diffusion facilitator / SLC30A) family transport zinc in the opposite direction, supplying organelles or exporting zinc from the cell. There are fourteen *Zip* and ten *ZnT* genes in the human genome, with functional specificity arising from a combination of restricted transcript expression and targeted protein localization [17, 18]. For instance, ZnT1 is localized to the basolateral PM of

intestinal enterocytes whereas ZnT8 is associated with insulin-containing granules in pancreatic β-cell islets.

We have been exploiting the molecular genetic tools available in the vinegar fly *Drosophila melanogaster* to investigate the cellular regulation of copper levels *in vivo* [19-25]. The fly genome encodes two main Ctr proteins, the constitutively-expressed Ctr1A, which is required for most cellular uptake and is essential for viability [26] and the inducible Ctr1B that is dispensable under normal conditions but needed under both copper starvation and copper toxicity conditions [27, 28]. Reduced copper in cuticle-secreting epidermal cells results in loss of pigmentation in adult *Drosophila* cuticle [19], presumably due to reduced activity of the copper-dependent laccase-2 enzyme [29].

Although copper-deficiency is just one possible cause of loss of pigmentation, we used this phenotype in a preliminary screen to identify novel genes that may be regulating cellular copper levels, making use of a genome-wide RNA interference (RNAi) screen performed previously [30]. We found that two genes, *vhaPPA1-2* and *bib*, were both needed for adult cuticle pigmentation and furthermore, that midgut-specific knockdown of these genes resulted in transcriptional up-regulation of *Ctr1B*, a known copper-deficiency response. *vhaPPA1-2* encodes one of fourteen subunits of the vacuolar-type H^+-ATPase (V-ATPase) complex [31], which transports H^+ protons into the lumen of the endosomes, helping acidify them as they mature from early to late stages [32, 33]. *bib* is the fly homologue of the mammalian water channel gene, *aquaporin 4* [34], although no evidence of water channel activity has been found for *bib* [35]. It was originally described as a neurogenic gene due to the neural hypertrophy seen in *bib* mutants [36], was found to augment the Delta-Notch signalling pathway [37], and has been shown to mediate cell-cell adhesion [35]. Here we explore the role that *vhaPPA1*-2 and *bib* play in the proper localization of the copper uptake transporters Ctr1A and Ctr1B and the zinc import protein dZip89B.

EXPERIMENTAL

Drosophila maintenance

All *Drosophila* strains and crosses were maintained on standard medium at 25°C unless stated otherwise. Standard medium was supplemented with either bathocuproinedisulfonic acid (BCS; Sigma Aldrich, St Louis, MO, USA) to make copper-deficient medium, copper sulphate ($CuSO_4$ Merck, Whitehouse Station, NJ, USA) to make copper-supplemented medium, zinc chloride ($ZnCl_2$) to make zinc-supplemented medium, or N,N,N',N'-tetrakis(2-pyridylmethyl)ethylenediamine (TPEN) to make zinc-deficient medium.

Drosophila stocks

Fly stocks used were w^{1118} (BL3605, Bloomington Drosophila Stock Center, Bloomington, IN, USA), *Elav-GAL4* ($Elav^{C155}$, BL6920) *Gmr-GAL4* (BL9146), *mex-GAL4* ([38]), *Pannier* (*Pnr*)*-GAL4* (BL3039), *HR-GAL4* (gift from P. Daborn [39]), *Ctr1B-EYFP* (gift from W. Schaffner, University of Zurich [27]) and PhiC31 attP-51C and attP-86Fb (gift from K. Basler, University of Zurich [40]). RNAi lines obtained from the Vienna Drosophila RNAi Center [41] were V48830 (*vhaPPA1-2*), V8993 (*bib*), V17102 (*vha68-1*), V25985 (*vha13*), V30384 (*vhaM9.7-b*), V34390 (*vha16-5*), V45377 (*vha26*), V47187 (*vhaPPA1-1*), V47471 (*vhaSFD*), V49290 (*vha16-1*), V46563 (*vha44*), V46553 (*vha55*) V8315 (*ATP7*) and V46757 (*Ctr1A*). Over expression lines *pUAST-Ctr1A*^{flag} and *pUAST-Ctr1B*^{flag} have been described previously [19].

Quantification of RNAi knockdown efficacy

mRNA was extracted using TRIzol Reagent (Life Technologies) from 20 6-day old larvae each from: 1) *Da-GAL4>+*; 2) *UAS-RNAi>+*; and 3) *Da-GAL4>UAS-RNAi* transgene combinations. cDNA were generated using SuperScript III First-Strand Synthesis System (Life Technologies). *bib* and *vhaPPA1-2* transcript levels were quantified by Real Time qPCR using the following primer pairs in combination with SYBR green on a Roche Lightcycler. Their relative expression was compared to the housekeeping gene *Rps20* using Rps20 primers (gift from R. Lee [42]).

vhappa1-2 RTF ATAATCTTCGCCAACGTGATGGTCA;

vhappa1-2 RTR CCGGACCACAGGAAGGGATT;
bib RTF ATCCACGGATCCCATGAAGAAGT;
bib RTR CCCATTTGTTAAGCACAAACGAAGGA;
rps20 F CCGCATCACCCTGACATCC;
rps20 R TGGTGATGCGAAGGGTCTTG.

Da-GAL4>bib^{RNAi} flies showed a >90% reduction in mRNA levels compared to both controls ($p = 0.001$). No significant reduction in *vhaPPA1-2* mRNA levels was observed, however basal *vhaPPA1-2* expression is extremely low [31] and a decrease from this low starting point may be beyond the sensitivity of our qPCR approach.

Cloning and generation of transgenic *Drosophila*

The *Drosophila* full-length *vhaPPA1-2* and *bib* open reading frames were PCR-amplified from cDNA extracted from *w*^{1118} 3rd instar larvae with the following primers:

vhaPPA1-2 forward, GGGGTACCATGATCTCTAAGATGAGTTTT;
vhaPPA1-2 reverse, GCTCTAGACTAATTAATGGTTTCCGCCTT;
bib forward, GGGGTACCATGGCCGACGAAAGTCTGCAC;
bib reverse, GCTCTAGATCAGTTGGGCCTCAGCGGCA.

The *vhaPPA1-2* and *bib* PCR fragments were subcloned in-frame with an N-terminal mCherry tag or without tag into the pUAST-attB vector. These constructs were injected into PhiC31 attP 51C and 86Fb fly lines. Microinjections utilised an Eppendorf Femtojet apparatus with Femtotips II (Eppendorf) prepulled glass needles.

Microscopy

Adult flies were partially dissected then mounted directly onto plasticine and monitored with a Leica MZ6 stereomicroscope. All images were recorded with a Leica DC300 digital camera using Leica Application Suite (LAS) software.

For observing *Ctr1B-eYFP* expression in the midgut, 3rd instar larvae were dissected in cold phosphate-buffered saline (PBS), then mounted directly in 50% glycerol and monitored with a Leica DMLB compound microscope.

For localization studies, salivary glands from wandering 3rd instar larvae were dissected in cold PBS then fixed for 30 minutes in 4% paraformaldehyde at room temperature. Tissues were stained with DAPI (20 μg/ml for 1 minute at room

temperature, Sigma) and Rhodamine Phalloidin (4 units/ml for 5 minutes at room temperature, Life Technologies, Carlsbad, CA, USA) to highlight the nucleus and PM respectively. Finally, the salivary glands were mounted onto glass slides in 70% glycerol. Monitoring and recording of eGFP or mCherry fluorescence was performed within 1 hour of dissection/mounting for optimal fluorescence signal. Fluorescence was detected using a Nikon C1 Upright confocal microscope and a x20 oil emersion objective lens. Excitation energies of 405 nm, 488 nm and 561 nm were used.

RESULTS

vhaPPA1-2 and *bib* are required for cuticle pigmentation

vhaPPA1-2 and *bib* were identified previously in a genome-wide RNAi screen as causing unspecified pigmentation defects in the adult cuticle when knocked down using *Pnr-GAL4*, which drives expression of UAS constructs in a broad stripe down the midline of the developing thorax and abdomen [30]. To determine the exact nature of the pigmentation defects, the same *vhaPPA1-2* and *bib* RNAi lines were again expressed under the control of *Pnr-GAL4*. Knockdown of *vhaPPA1-2* resulted in a mild but detectable hypo-pigmentation on the midline of the adult thorax (Fig. 1B) compared to wild type (Fig. 1A). Knockdown of *bib* resulted in a stronger hypo-pigmentation in the adult thorax and abdomen (Fig. 1C). qPCR showed that ubiquitous knockdown (using *Da-GAL4*) reduced *bib* mRNA levels by >90% compared to controls, however no significant reduction in *vhaPPA1-2* transcript levels was observed, possibly due to the previously reported minimal basal expression levels of this gene [31] and insufficient sensitivity of the qPCR assay used.

To confirm that the hypo-pigmentation phenotype observed by suppressing *vhaPPA1-2* is due to disruption of the V-ATPase complex, genes encoding an additional 11 of the 14 subunits of the complex were knocked down. In five cases, *vha68-1, vhaM9.7-b, vha16-5, vha44* or *vhaSFD*, knockdown using *Pnr-GAL4* resulted in phenotypes stronger than those seen with *vhaPPA1-2*, exemplified by the strong thoracic cleft and moderate abdominal hypo-pigmentation caused by knockdown of *vha44* (Fig. 1D). Knockdown of *vha13*, *vha68-2*, *vha26*, *vha55* and *vhaPPA1-1* or *vha16-1* resulted in lethality, therefore the effect on pigmentation could not be determined.

Knockdown of *vhaPPA1-2* modifies copper deficiency and toxicity phenotypes in the adult eye

To determine if the cuticle pigmentation defects caused by *vha* and *bib* knockdown could be due to altered copper metabolism, genetic interaction experiments were carried out. The loss of pigmentation caused by suppressing *vhaPPA1-2* or *bib* could not be rescued by over-expressing the copper uptake genes *Ctr1A* or *Ctr1B* (Fig. S1A – D).

To investigate if *vhaPPA1-2* and *bib* were required for copper uptake, co-knockdown analyses were carried out in the fly eye, which requires *Ctr1A* activity for its development [19]. Compared to the wild type eye (Fig. 2A), knockdown of *Ctr1A* alone under *Gmr-GAL4* control resulted in a smaller, flatter eye of irregular shape with a characteristic pit in the centre, as shown previously (Fig. 2B, [19]). Knockdown of *vhaPPA1-2* alone had no phenotypic effect (Fig. 2C). Co-knockdown of *vhaPPA1-2* enhanced the *Ctr1A* sunken eye phenotype resulting in an even smaller, flatter eye (Fig. 2D), indicating that loss of *vhaPPA1-2* exacerbates the copper deficiency caused by *Ctr1A* knockdown. Knockdown of *bib* alone resulted in a smaller eye with disrupted ommatidial array (Fig. 2E). When *bib* was co-suppressed with *Ctr1A*, the resultant eyes showed an additive phenotype with features of both *Ctr1A* and *bib* knockdown (Fig. 2F).

To determine if knockdown of *vhaPPA1-2* or *bib* could modify a copper toxicity phenotype, *Ctr1A* was over-expressed in the eye together with knockdown of the copper efflux gene *ATP7* [19] which resulted in a smaller, rough and sunken eye in males, as shown previously (Fig. 2G, [19]). Knockdown of *vhaPPA1-2* in the male eye completely rescued the copper toxicity eye phenotype (Fig. 2H). This phenotype was not rescued by suppressing *bib* in the eye (Fig. 2I), but *bib* knockdown itself caused a rough eye phenotype (Fig. 2E).

Knockdown of *vhaPPA1-2* or *bib* in the larval midgut causes induction of *Ctr1B*, indicating reduced cellular copper levels

Looking for additional evidence of a role for *vhaPPA1*-2 or *bib* in copper homeostasis, we turned to the larval midgut, where *Ctr1B* transcription is induced under low-copper conditions [27]. Under normal food (NF) conditions, a *Ctr1B-eYFP* reporter line [27] was expressed in a section of the midgut posterior to the copper cells (CC) in the 3rd instar larval midgut (Fig. 3A, [27]). Expression of *Ctr1B-eYFP* was strongly induced throughout the midgut when the larvae were grown on food supplemented with the copper chelator BCS (Fig. 3B, [27]), indicating an up-regulation of *Ctr1B* expression in copper-depleted cells. Under NF conditions, knockdown of *vhaPPA1-2* using the midgut-specific driver *HR-GAL4* [39] resulted in a mild increase in the extent and intensity of *Ctr1B-eYFP* expression in its basal expression domain (Fig. 3C). Knockdown of *bib* resulted in a stronger increase in *Ctr1B-eYFP* expression in

this domain and additional expression in the anterior-most portion of the midgut (Fig. 3D). These results suggested that both *vhaPPA1*-2 and *bib* were required for optimal copper accumulation in at least some midgut cells. Midgut knockdown of *vhaPPA1*-2 or *bib* did not affect the survival of these larvae, indicating that this mild reduction in copper accumulation was not detrimental to the fly.

vhaPPA1-2 and _bib_ are required for the proper localization of copper and zinc transporters

The adult and larval phenotypes described above were consistent with a decrease in cellular copper accumulation and could be due to a change in the localization of one of the key copper uptake proteins. Therefore, the localization of ectopically expressed Ctr1A- and Ctr1B-eGFP fusion proteins was investigated in larval salivary gland cells, using *Elav-Gal4* which drives salivary gland as well as pan-neuronal expression. Ctr1A- and Ctr1B-eGFP normally localized to the apical membrane (Fig. 4A and 4E respectively) with Ctr1A-eGFP also showing sub-apical intracellular clusters (Fig. 4A). Knockdown of *vhaPPA1-2* resulted in a loss of apical PM Ctr1A-eGFP, which was replaced by large intracellular accumulations (Fig. 4B). Ctr1A-eGFP was similarly affected by loss of *bib* although some was retained at the PM (Fig. 4C). Knockdown of a second V-ATPase subunit, *vha55*, caused a more marked loss of apical Ctr1A-eGFP with numerous intracellular accumulations seen (Fig. 4D). Ctr1B-eGFP behaved in a similar fashion to Ctr1A-eGFP, becoming completely internalized by knockdown of *vhaPPA1-2* (Fig. 4F) or *vha55* (Fig. 4H) while continuing to partially overlap with apical phalloidin under *bib* knockdown (Fig. 4G*)*.

In each case above, the morphology of the salivary gland cells was severely disorganized by knockdown of *vhaPPA1-2*, *bib* or *vha55* although viable adults emerged from these crosses. To determine if the mis-localization of Ctr1A- and Ctr1B-eGFP was due to a general disruption of salivary gland cells' PM, the membrane marker CD8-GFP was examined. CD8-GFP normally showed strong localization to both apical and basolateral PMs (Fig. 4I). Under *vhaPPA1-2* knockdown, the apical PM and the salivary gland lumen were no longer detectable and the basolateral PM was disorganized, with an increase in intracellular CD8-GFP visible (Fig. 4J). *bib* knockdown had a less dramatic impact, with the lumen and apical PM still detectable despite strong morphological defects (Fig. 4K). Knockdown

of *vha55* had the strongest effect, almost completely removing both apical and basolateral CD8-GFP, with a mixture of diffuse and punctate intracellular GFP signal remaining (Fig. 4L).

The disruption of CD8-GFP localization indicated that inhibition of V-ATPase or Bib activity had a more general effect on membrane organization and was not specific to the copper uptake transporters. Therefore, the localization of dZip89B-eGFP, a zinc uptake transporter that localized to the apical PM of the salivary glands (Figure 4M) was also investigated. Knockdown of *vhaPPA1*-2, *bib* or *vha55* resulted in a mis-localization of dZip89B-eGFP (Fig. 4N, O and P respectively) similar to that seen for Ctr1A- and Ctr1B-eGFP.

To determine if other cellular membranes were also disrupted, the localization of the copper efflux protein ATP7 was investigated. Under the control of *Elav-GAL4*, mCherry-ATP7 localized to the basolateral PM (Fig. 5A). Knockdown of *vhaPPA1-2* caused an internalization of mCherry-ATP7 with subsequent loss of the basolateral signal (Fig. 5B). *bib* knockdown had a milder effect, with considerable basolateral mCherry-ATP7 retained (Fig. 5C) while *vha55* knockdown again had the most dramatic effect, resulting in complete redistribution of mCherry-ATP7 to large punctate intracellular structures (Fig. 5D). These results indicated that mis-localization of membrane proteins by knockdown of *vhaPPA1-2*, *bib* or *vha55* was not limited to apically localized proteins.

VHAPPA1-2 and Bib co-localize with Ctr1A and Ctr1B

To test whether the copper transporters may be localized to the same cellular membranes as VHAPPA1-2 or Bib, over-expression constructs containing an in-frame N-terminal mCherry fluorescent fusion protein were generated and ectopically expressed under *Elav-GAL4* control. mCherry-VHAPPA1-2 was distributed in a web-like pattern throughout the cell with occasional punctate concentrations observed near the nuclei (Fig. 6B) while mCherry-Bib showed strong localization to the apical PM as well as large accumulations within the cell (Fig. 6C).

mCherry-VHAPPA1-2 showed extensive co-localization with the punctate intracellular portion of Ctr1A-eGFP (Fig. 6D). Co-expression of Ctr1B-eGFP with mCherry-VHAPPA1-2 lead to indistinct intracellular accumulations of Ctr1B-eGFP

not normally observed, while mCherry-VHAPPA1-2 also became more diffuse and indistinct (Fig. 6E). Ctr1A-eGFP co-localized with mCherry-Bib both at the apical PM and at large sub-apical clusters (Fig. 6F). The intracellular portion of mCherry-Bib also co-localized with Ctr1B-eGFP (Fig. 6G) which again showed intracellular signal not normally present.

Midgut-specific knockdown of *bib* increases tolerance to dietary zinc

Since knockdown of *vhaPPA1*-2 or *bib* disrupted the localization of key metal transport proteins, we tested whether this would lead to an altered tolerance to dietary metals or metal ion depletion. Using the midgut-specific driver *mex-GAL4, vhaPPA1-2* and *bib* were suppressed and 1st instar larvae were placed on food with different $CuSO_4$, $ZnCl_2$, BCS (copper chelator) and TPEN (zinc chelator) concentrations, with survival to adulthood assessed. Knockdown of *vhaPPA1-2* caused a moderate but significant decrease in survival even on the normal food (NF) control media but resulted in dramatically increased susceptibility to TPEN food (Fig. 7). *bib* knockdown had no effect on survival on normal food but caused significantly increased resistance to dietary zinc, particularly at 12 mM $ZnCl_2$ and increased susceptibility to 100 μM TPEN (Fig. 7).

DISCUSSION

Correct localization of metal ion transporters is essential for their function. In a search for novel copper homeostasis genes, we identified *vhaPPA1-2* and *bib* as being required for optimal copper accumulation. RNAi knockdown of these genes caused typical copper deficiency phenotypes; adult cuticle hypo-pigmentation and *Ctr1B* induction in the larval midgut. Furthermore *vhaPPA1-2* knockdown could suppress copper toxicity and enhance copper deficiency phenotypes in the adult eye. However, a detailed examination of the effect of *vha* and *bib* knockdown on the localization of several different metal ion transport proteins and membrane markers revealed that these genes are playing important roles in the general maintenance of epithelial cell shape and polarity and that ion transport proteins are also susceptible to their loss of function.

All proteins tested here, whether located apically or basolaterally, were affected by *vhaPPA1-2* and *vha55* knockdown, indicating that these genes are not acting specifically in copper or zinc homeostasis but rather are playing a more generic role in cell membrane maintenance. The 14 subunits of the *Drosophila* V-ATPase complex are encoded by a total of 33 genes [31]. Loss-of-function mutations in 10 of these genes are homozygous lethal and display a transparent malpighian tubule phenotype suggested to be a defect in urinary acidification [31]. Mutants of the neural-specific V-ATPase subunit *vhaAC39* have been found to phenocopy *Rabconnectin-3alpha* and *beta* mutants, causing defects in endocytic trafficking that result in the accumulation of membrane proteins such as Notch in the late endosome, indicating that acidification of the endosomal compartment is essential for proper Notch signalling [43]. Furthermore, mutations in *vha100-1* lead to vesicle accumulation in synaptic terminals, the VHA100-1 protein co-localizing with synaptic vesicles [44]. The VhaPRR subunit of the V-ATPase is also required for the correct function of the Frizzled receptor in the Wingless and Planar Cell Polarity pathways [45], and for endolysosomal sorting and degradation of membrane proteins such as E-Cadherin and the Notch [46].

Our results suggest that *vhaPPA1-2* and *vha55* both contribute to a role of the V-ATPase in endocytic trafficking in non-neuronal epithelial cells and that both copper and zinc uptake proteins require this function for optimal metal ion import.

Supporting this notion, mutation of the *V0 subunit 4* in zebrafish resulted in sensitivity to copper deficiency, with the copper chelator Neocuproine eliciting cell-autonomous loss of melanin and wavy notochord phenotypes attributed to a reduction in cuproenzyme activity [47]. These phenotypes were exacerbated by reduction in *ATP7a* function without cytochrome C oxidase activity being affected, leading the authors to propose that either: 1) acidification via the V-ATPase is required for incorporation of copper into secretory pathway cuproenzymes; or 2) a V-ATPase mediated proton gradient is needed for copper transport across membranes. Our data raises a third option, that V-ATPase activity is required more generally for endosome recycling and that metal ion transport proteins are particularly sensitive to disruptions to this process.

Knockdown of *bib* also had a deleterious effect on salivary gland morphology and a similar mis-localization effect on the three metal uptake proteins studied. The extensive co-localization between Bib, Ctr1A and Ctr1B, both in intracellular vesicles and on the apical PM, indicated these proteins reside in the same subcellular compartments. In *Drosophila* embryos, endogenous Bib had previously been seen by electron microscopy both at the PM where it is concentrated at adherens junctions and in small intracellular vesicles [37]. Bib has also been found to co-localize with endosomal proteins [48]. The co-localization of Bib with Ctr1A and Ctr1B, combined with the effect of *bib* knockdown, lead us to favour a model where *bib* is needed for correct endosome maturation and in its absence, the copper and zinc transporters are not recycled efficiently back to the apical cell surface, leading to a reduction in metal ion uptake. We cannot discount alternative possibilities such as an adhesion role for *bib* [35] but the impressive increase in zinc tolerance imparted by *bib* knockdown in the midgut indicates that reduction in midgut Bib activity, while not being detrimental to overall animal health, has a particularly strong influence on zinc uptake.

The results presented here implicate Bib and the V-ATPase complex in the general maintenance of epithelial cell polarity and membrane structure, possibly via the endosome recycling pathway as previously suggested. Differences in phenotypes caused by knockdown of *bib* or *V-ATPase* components indicate they are not playing identical roles and while the role for the V-ATPase in endosome acidification is well-characterized, the precise function of Bib in the endosome remains elusive. Nonetheless, our work demonstrates that metal ion transport is particularly sensitive

to disruptions in plasma membrane structure or function because under RNAi knockdown of *bib* or *V-ATPase* components, overall animal viability is not affected yet metal-specific phenotypes such as cuticle pigmentation, reporter-gene expression and metal ion tolerance are revealed.

ACKNOWLEDGEMENTS

Drosophila stocks were imported into Australia by The Australian Drosophila Biomedical Research Support Facility (www.ozdros.com). All *Drosophila* RNAi lines were provided by Vienna Drosophila RNAi Centre. Confocal microscopy was carried out at Monash Micro Imaging, who also provided training and technical support. This research was supported by a Project Grant (RB #606609) from the Australian National Health and Medical Research Council. All transgenic *Drosophila* experiments carried out in this research were performed with the approval of the Monash University Institutional Biosafety Committee.

REFERENCES

1. Linder, M.C. and M. Hazegh-Azam, *Copper biochemistry and molecular biology.* Am J Clin Nutr, 1996. **63**(5): p. 797S-811S.
2. Andreini, C., et al., *Counting the zinc-proteins encoded in the human genome.* J Proteome Res, 2006. **5**(1): p. 196-201.
3. Miller, J., A.D. McLachlan, and A. Klug, *Repetitive zinc-binding domains in the protein transcription factor IIIA from Xenopus oocytes.* Embo J, 1985. **4**(6): p. 1609-14.
4. Coleman, J.E., *Structure and mechanism of alkaline phosphatase.* Annu Rev Biophys Biomol Struct, 1992. **21**: p. 441-83.
5. Malemud, C.J., *Matrix metalloproteinases (MMPs) in health and disease: an overview.* Front Biosci, 2006. **11**: p. 1696-701.
6. Coyle, P., et al., *Metallothionein: the multipurpose protein.* Cell Mol Life Sci, 2002. **59**(4): p. 627-47.
7. Egli, D., et al., *A family knockout of all four Drosophila metallothioneins reveals a central role in copper homeostasis and detoxification.* Mol Cell Biol, 2006. **26**(6): p. 2286-96.
8. Kim, B.E., T. Nevitt, and D.J. Thiele, *Mechanisms for copper acquisition, distribution and regulation.* Nat Chem Biol, 2008. **4**(3): p. 176-85.
9. Aller, S.G. and V.M. Unger, *Projection structure of the human copper transporter CTR1 at 6-A resolution reveals a compact trimer with a novel channel-like architecture.* Proc Natl Acad Sci U S A, 2006. **103**(10): p. 3627-32.
10. De Feo, C.J., et al., *Three-dimensional structure of the human copper transporter hCTR1.* Proc Natl Acad Sci U S A, 2009. **106**(11): p. 4237-42.
11. Zhou, B. and J. Gitschier, *hCTR1: a human gene for copper uptake identified by complementation in yeast.* Proc Natl Acad Sci U S A, 1997. **94**(14): p. 7481-6.
12. Petris, M.J., et al., *Copper-stimulated Endocytosis and Degradation of the Human Copper Transporter, hCtr1.* J. Biol. Chem., 2003. **278**(11): p. 9639-9646.
13. Eisses, J.F., Y. Chi, and J.H. Kaplan, *Stable plasma membrane levels of hCTR1 mediate cellular copper uptake.* J Biol Chem, 2005. **280**(10): p. 9635-9.
14. Klomp, A.E., et al., *Biochemical characterization and subcellular localization of human copper transporter 1 (hCTR1).* Biochem J, 2002. **364**(Pt 2): p. 497-505.
15. Voskoboinik, I., J. Camakaris, and J.F. Mercer, *Understanding the mechanism and function of copper P-type ATPases.* Adv Protein Chem, 2002. **60**: p. 123-50.
16. Veldhuis, N.A., et al., *The multi-layered regulation of copper translocating P-type ATPases.* Biometals, 2009. **22**(1): p. 177-90.
17. Cousins, R.J., J.P. Liuzzi, and L.A. Lichten, *Mammalian zinc transport, trafficking, and signals.* J Biol Chem, 2006. **281**(34): p. 24085-9.
18. Eide, D.J., *Zinc transporters and the cellular trafficking of zinc.* Biochim Biophys Acta, 2006. **1763**(7): p. 711-22.
19. Binks, T., et al., *Tissue-specific interplay between copper uptake and efflux in Drosophila.* J Biol Inorg Chem, 2010. **15**(4): p. 621-8.
20. Burke, R., E. Commons, and J. Camakaris, *Expression and localisation of the essential copper transporter DmATP7 in Drosophila neuronal and intestinal tissues.* Int J Biochem Cell Biol, 2008. **40**(9): p. 1850-60.
21. Lye, J.C., et al., *Detection of genetically altered copper levels in Drosophila tissues by synchrotron x-ray fluorescence microscopy.* PLoS One, 2011. **6**(10): p. e26867.
22. Norgate, M., et al., *Essential roles in development and pigmentation for the Drosophila copper transporter DmATP7.* Mol Biol Cell, 2006. **17**(1): p. 475-84.
23. Norgate, M., et al., *Syntaxin 5 is required for copper homeostasis in Drosophila and mammals.* PLoS One, 2010. **5**(12): p. e14303.

24. Southon, A., et al., *Copper homoeostasis in Drosophila melanogaster S2 cells.* Biochem J, 2004. **383**(Pt 2): p. 303-9.
25. Southon, A., et al., *Malvolio is a copper transporter in Drosophila melanogaster.* J Exp Biol, 2008. **211**(Pt 5): p. 709-16.
26. Turski, M.L. and D.J. Thiele, *Drosophila Ctr1A functions as a copper transporter essential for development.* J Biol Chem, 2007. **282**(33): p. 24017-26.
27. Selvaraj, A., et al., *Metal-responsive transcription factor (MTF-1) handles both extremes, copper load and copper starvation, by activating different genes.* Genes Dev, 2005. **19**(8): p. 891-6.
28. Zhou, H., K.M. Cadigan, and D.J. Thiele, *A Copper-regulated Transporter Required for Copper Acquisition, Pigmentation, and Specific Stages of Development in Drosophila melanogaster.* J. Biol. Chem., 2003. **278**(48): p. 48210-48218.
29. Riedel, F., D. Vorkel, and S. Eaton, *Megalin-dependent yellow endocytosis restricts melanization in the Drosophila cuticle.* Development, 2011. **138**(1): p. 149-58.
30. Mummery-Widmer, J.L., et al., *Genome-wide analysis of Notch signalling in Drosophila by transgenic RNAi.* Nature, 2009. **458**(7241): p. 987-92.
31. Allan, A.K., et al., *Genome-wide survey of V-ATPase genes in Drosophila reveals a conserved renal phenotype for lethal alleles.* Physiol Genomics, 2005. **22**(2): p. 128-38.
32. Huotari, J. and A. Helenius, *Endosome maturation.* EMBO J, 2011. **30**(17): p. 3481-500.
33. Nishi, T. and M. Forgac, *The vacuolar (H+)-ATPases--nature's most versatile proton pumps.* Nat Rev Mol Cell Biol, 2002. **3**(2): p. 94-103.
34. Rao, Y., L.Y. Jan, and Y.N. Jan, *Similarity of the product of the Drosophila neurogenic gene big brain to transmembrane channel proteins.* Nature, 1990. **345**(6271): p. 163-7.
35. Tatsumi, K., et al., *Drosophila big brain does not act as a water channel, but mediates cell adhesion.* FEBS Lett, 2009. **583**(12): p. 2077-82.
36. Rao, Y., et al., *The big brain gene of Drosophila functions to control the number of neuronal precursors in the peripheral nervous system.* Development, 1992. **116**(1): p. 31-40.
37. Doherty, D., L.Y. Jan, and Y.N. Jan, *The Drosophila neurogenic gene big brain, which encodes a membrane-associated protein, acts cell autonomously and can act synergistically with Notch and Delta.* Development, 1997. **124**(19): p. 3881-93.
38. Phillips, M.D. and G.H. Thomas, *Brush border spectrin is required for early endosome recycling in Drosophila.* J Cell Sci, 2006. **119**(Pt 7): p. 1361-70.
39. Chung, H., et al., *Cis-regulatory elements in the Accord retrotransposon result in tissue-specific expression of the Drosophila melanogaster insecticide resistance gene Cyp6g1.* Genetics, 2007. **175**(3): p. 1071-7.
40. Bischof, J., et al., *An optimized transgenesis system for Drosophila using germ-line-specific phiC31 integrases.* Proc Natl Acad Sci U S A, 2007. **104**(9): p. 3312-7.
41. Dietzl, G., et al., *A genome-wide transgenic RNAi library for conditional gene inactivation in Drosophila.* Nature, 2007. **448**(7150): p. 151-6.
42. Colinet, H., S.F. Lee, and A. Hoffmann, *Temporal expression of heat shock genes during cold stress and recovery from chill coma in adult Drosophila melanogaster.* FEBS J, 2010. **277**(1): p. 174-85.
43. Yan, Y., N. Denef, and T. Schupbach, *The vacuolar proton pump, V-ATPase, is required for notch signaling and endosomal trafficking in Drosophila.* Dev Cell, 2009. **17**(3): p. 387-402.
44. Hiesinger, P.R., et al., *The v-ATPase V0 subunit a1 is required for a late step in synaptic vesicle exocytosis in Drosophila.* Cell, 2005. **121**(4): p. 607-20.

45. Hermle, T., et al., *Regulation of Frizzled-dependent planar polarity signaling by a V-ATPase subunit.* Curr Biol, 2010. **20**(14): p. 1269-76.
46. Hermle, T., et al., *Drosophila ATP6AP2/VhaPRR functions both as a novel planar cell polarity core protein and a regulator of endosomal trafficking.* EMBO J, 2013. **32**(2): p. 245-59.
47. Madsen, E.C. and J.D. Gitlin, *Zebrafish mutants calamity and catastrophe define critical pathways of gene-nutrient interactions in developmental copper metabolism.* PLoS Genet, 2008. **4**(11): p. e1000261.
48. Kanwar, R. and M.E. Fortini, *The big brain aquaporin is required for endosome maturation and notch receptor trafficking.* Cell, 2008. **133**(5): p. 852-63.

FIGURE LEGENDS

Figure 1: Knockdown of *vhaPPA1-2, vha44* and *bib* cause hypo-pigmentation phenotypes in the *Drosophila* adult cuticle. Dorsal views of the female adult *Drosophila* thorax / abdomen, shown anterior to the top. For each of the genotypes shown in this and subsequent figures, images are representative of > 10 individuals. kd = RNAi knockdown. All flies have *Pnr-GAL4* which drives UAS expression in the middle ~50% of the thorax and abdomen. A) Wild type fly with *Pnr-GAL4* showing normal pigmentation on the thorax (th), scuttelum (sc) and abdomen (ab) - approximate borders of the *Pnr* expression domain are shown with red lines. B) *Pnr-GAL4>UAS-vhaPPA1-2^{RNAi}* fly showing mild hypo-pigmentation on the midline of the thorax. C) *Pnr-GAL4>UAS-bib^{RNAi}* fly showing, in the central *Pnr* domain, stronger hypo-pigmentation in the anterior thorax and abdomen and a dark patch on the posterior thorax. D) *Pnr-GAL4>UAS-vha44^{RNAi}* fly showing a thoracic cleft, loss of scutellum and mild abdominal hypo-pigmentation in the *Pnr* domain. Scale bar = 200 μm.

Figure 2. *vhaPPA1-2* knockdown modifies copper deficiency and toxicity phenotypes. Adult male *Drosophila* eyes, all with *Gmr-GAL4*, shown anterior to the left. A) Wild type *Gmr-GAL4>+* adult eye showing the normal oval shape and ordered ommatidial array. B) Eye from a *Gmr-GAL4>UAS-Ctr1A^{RNAi}* fly. The eye is smaller and flatter than normal, with irregular shape and a characteristic central pit. C) Eye from a *Gmr-GAL4>UAS-vhaPPA1-2^{RNAi}* fly appears completely wild type in shape, size and pattern. D) Eye from a *Gmr-GAL4>UAS-Ctr1A^{RNAi}; UAS-vhaPPA1-2^{RNAi}* fly is considerably smaller than the *Ctr1A* knockdown eye with more irregular shape. E) Eye from a *Gmr-GAL4>UAS-bib^{RNAi}* fly is smaller than wild type with irregular ommatidial patterning and an increased number of inter-ommatidial bristles. F) Eye from a *Gmr-GAL4>UAS-Ctr1A^{RNAi}; UAS-bib^{RNAi}* fly shows features of both *Ctr1A* and *bib* knockdown. G) Eye from a *Gmr-GAL4>UAS-ATP7^{RNAi}; UAS-Ctr1A^{flag}* fly. Increased copper levels result in this eye phenotype; eye has a glazed appearance, particularly in the central portion which is also sunken. H) Eye from a *Gmr-GAL4>UAS-ATP7^{RNAi}; UAS-Ctr1A^{flag}*; UAS-*vhaPPA1-2^{RNAi}* fly. Co-knockdown of *vhaPPA1-2* completely rescues the copper toxicity phenotype back to wild type. I)

Eye from a *Gmr-GAL4>UAS-ATP7*^{RNAi}*; UAS-Ctr1A*^{flag}; *UAS-bib*^{RNAi} fly. The copper toxicity phenotype appears exacerbated with an overall glazed appearance and patchy loss of eye pigmentation. Scale bar = 100 μm.

Figure 3. Knockdown of *vhaPPA1-2* and *bib* induces expression of a *Ctr1B-eYFP* reporter in the larval midgut. Each panel shows 3rd larval instar midguts containing the *Ctr1B-eYFP* reporter line and *HR-GAL4*, anterior to the left. A) Wild type larvae showing basal, un-induced *Ctr1B-eYFP* expression (green) in a small subset of midgut cells (arrow) posterior to the copper cells (cc). Yellow colour seen throughout the entire midgut is auto fluorescence from the gut contents. B) Wild type larvae raised on 300 μM BCS, showing extensive induction of *Ctr1B-eYFP* in most regions of the midgut. C) Knockdown of *vhaPPA1-2* under *HR-GAL4* control in the entire midgut in larvae raised on normal food (NF). Mild induction of *Ctr1B-eYFP* is seen as an expansion of the basal expression domain posterior to the copper cells (arrows). D) Knockdown of *bib* under *HR-GAL4* control in the entire midgut in larvae raised on normal food (NF). *Ctr1B-eYFP* expression is induced in cells of the gastric caecum (gc), copper cell (cc) region and in the basal expression domain posterior to the copper cells (arrows). Scale bar = 1 mm.

Figure 4. *vhaPPA1-2* and *bib* are required for correct localization of apical proteins. Salivary glands dissected from wandering 3rd instar larvae expressing various eGFP fusion proteins under *Elav-GAL4* control. In each, left panel shows eGFP fusion protein in green, middle panel shows phalloidin stain in red, and right panel shows merge of both together with nuclear DAPI signal in blue. A) Ctr1A-eGFP is concentrated on the apical PM that lines the lumen of the salivary gland. Some punctate intracellular Ctr1A-eGFP is also present. B - D) Ctr1A-eGFP together with knockdown of: B) *vhaPPA1-2*; C) *bib*; and D) *vha55*. E) Ctr1B-eGFP is located exclusively on the apical PM. F - H) Ctr1B-eGFP together with knockdown of: F) *vhaPPA1-2*; G) *bib*; and H) *vha55*. I) CDB-GFP is localized to both the apical PM and the external basolateral PM. J - L) CD8-GFP together with knockdown of: J) *vhaPPA1-2*; K) *bib*; and L) *vha55*. M) dZip89B-eGFP is localized exclusively on the apical PM. N - P) dZip89B-eGFP together with knockdown of: N) *vhaPPA1-2*; O) *bib*; and P) *vha55*. Scale bar = 100 μm.

Figure 5. *vhaPPA1-2* and *bib* are also required for correct localization of basolateral ATP7. Salivary glands expressing mCherry-ATP7 fusion protein under *Elav-GAL4* control. In each, left panel shows mCherry-ATP7 alone in red, right panel shows merge with nuclear DAPI signal in blue. A) Wild type salivary gland showing mCherry-ATP7 localized predominantly on the external basolateral PM of each cell. B - D) mCherry-ATP7 together with knockdown of: B) *vhaPPA1-2*; C) *bib*; and D) *vha55*. Scale bar = 100 μm.

Figure 6. Ctr1A and Ctr1B co-localize with VHAPPA1-2 and Bib. Salivary glands expressing various eGFP and mCherry fusion proteins under *Elav-GAL4* control. A) CD8-GFP localizes both to the lumenal apical PM and to the external basolateral PM. B) mCherry-VHAPPA1-2 is seen as a diffuse, web-like intracellular signal throughout each cell. C) mCherry-Bib is located predominantly at the apical PM, with additional punctate intracellular accumulations. D–G) Co-localization between copper transporters and VHAPPA1-2 / Bib. In each, left panel shows eGFP fusion protein in green, middle panel shows mCherry fusion protein in red, and right panel shows merge of both together with nuclear DAPI signal in blue. D) Ctr1A-eGFP with mCherry-VHAPPA1-2. E) Ctr1B-eGFP with mCherry-VHAPPA1-2. F) Ctr1A-eGFP with mCherry-Bib. G) Ctr1B-eGFP with mCherry-Bib. Scale bar = 100 μm.

Figure 7. Survival of *Drosophila* with dietary metal ion excess or deficiency. Percentage survival to adulthood of *Drosophila* 1st instar larvae transferred to food media supplemented with $CuSO_4$, the copper chelator BCS, $ZnCl_2$ or the zinc chelator TPEN. A) In each dietary condition, survival of *Mex-GAL4>vhaPPA1-2* or *bib* knockdown flies is normalized to the *Mex-GAL4>w^{1118}* control. On normal media (NF), the survival rate is reduced in *vhaPPA1-2* knockdown, but not *bib* knockdown flies, and the same is seen on 300 μM and 500 μM BCS. There is no effect on survival for *vhaPPA1-2* knockdown on either $CuSO_4$ or $ZnCl_2$ supplemented food, but the survival rate of *bib* knockdown flies is increased compared to wild type controls when supplemented with 8 mM (A) or 12 mM $ZnCl_2$ (B). A significant drop in survival for *vhaPPA1-2* knockdown flies was observed when supplemented with 50

μM to 150 μM TPEN. B) The 12 mM $ZnCl_2$ results are shown together with the NF control on a separate graph with different Y axis so as not to dwarf all the other results shown in (A). Each bar represents the mean of 4 to 5 experiments normalized to the wild type *w1118* control ± SE, 50 larvae per experiment (**p<0.01, ***p<0.001).

FIGURE 1

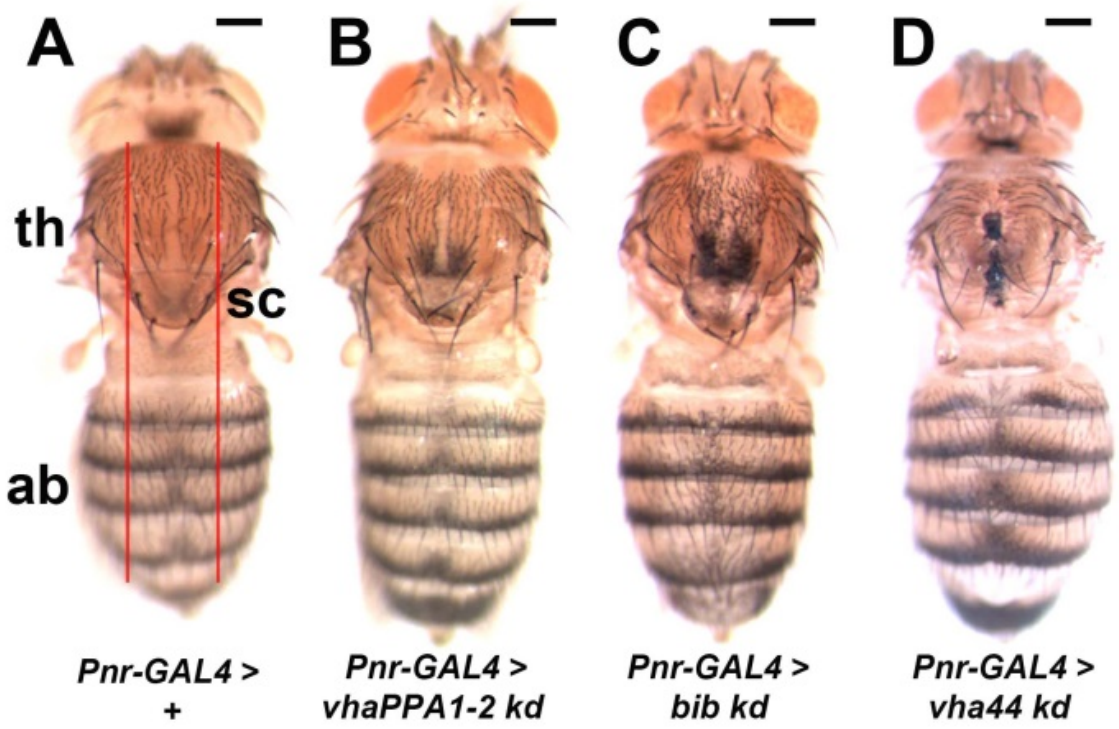

FIGURE 2

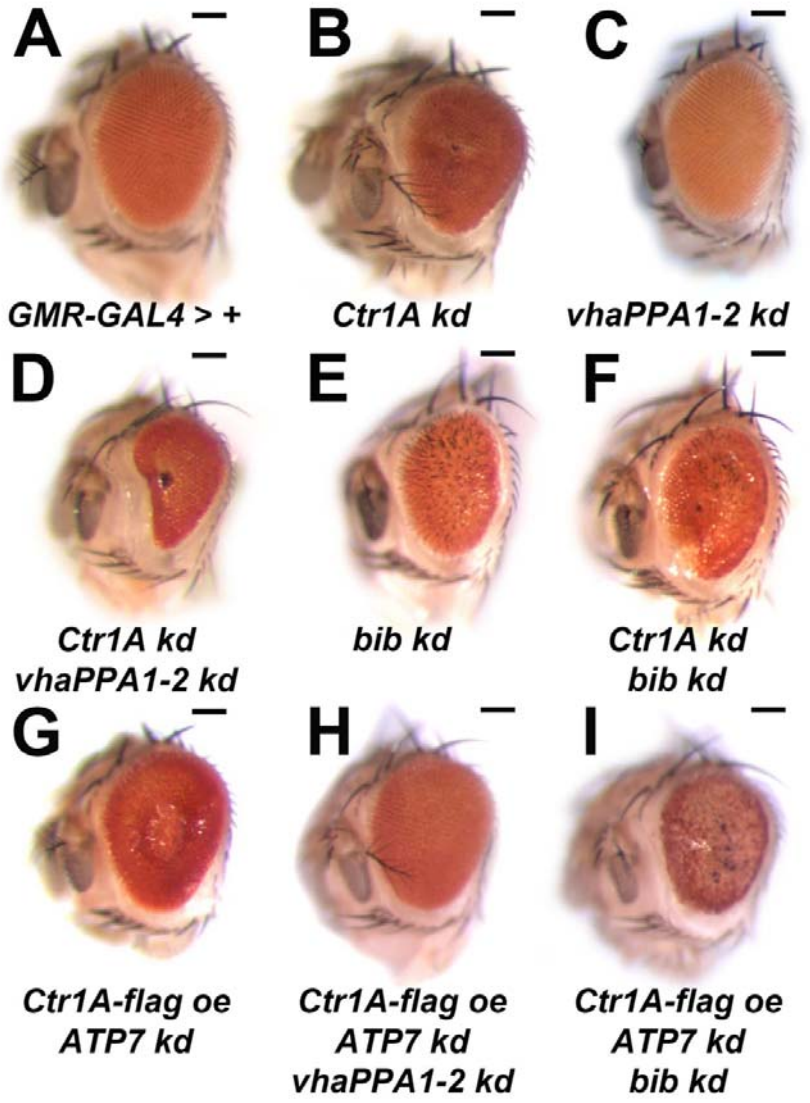

FIGURE 3

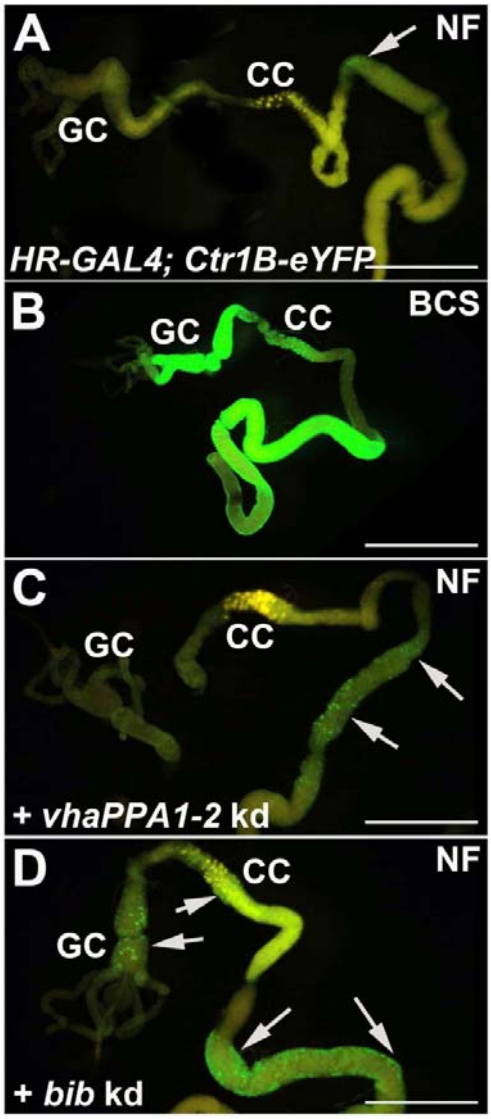

FIGURE 4

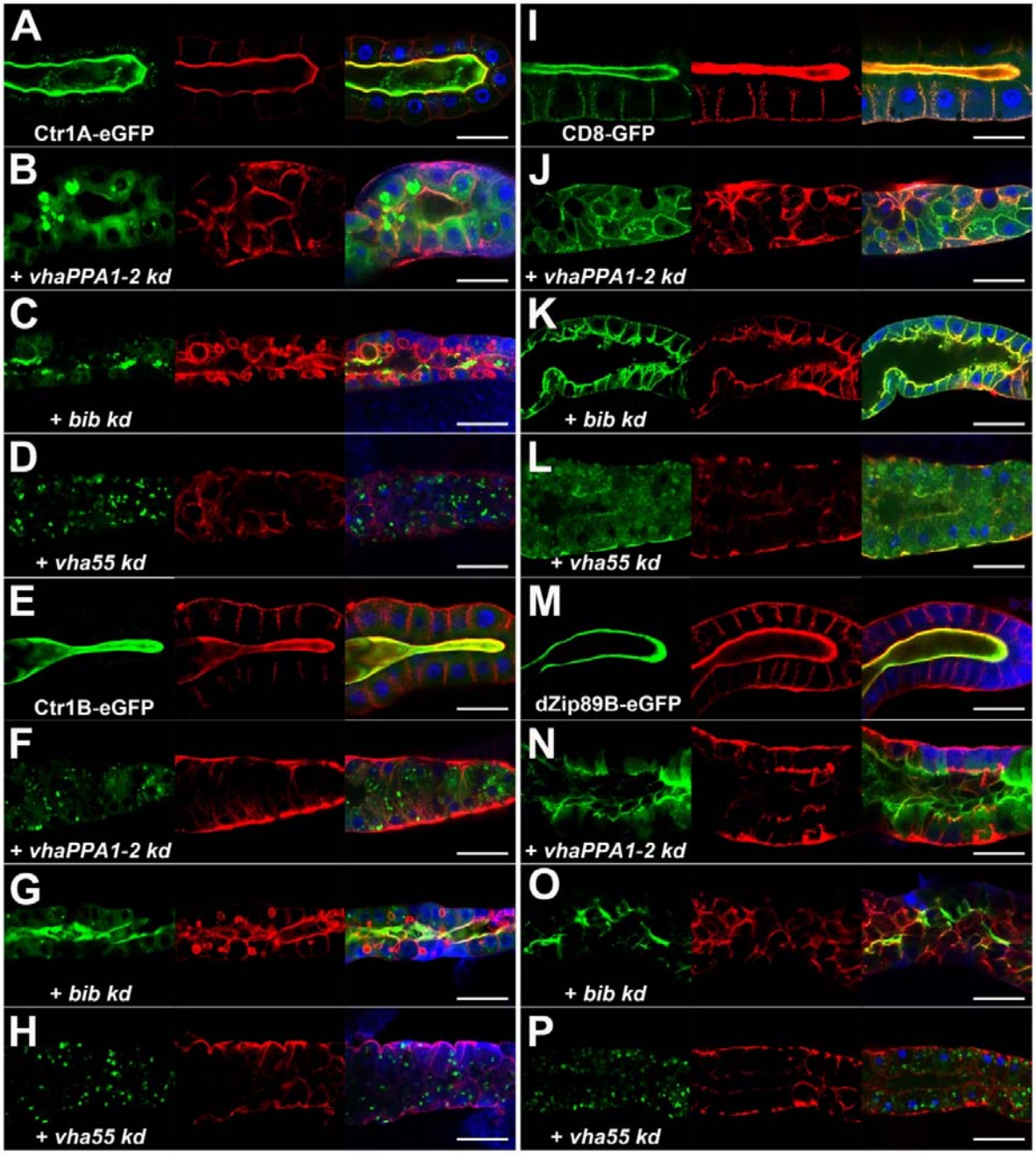

FIGURE 5

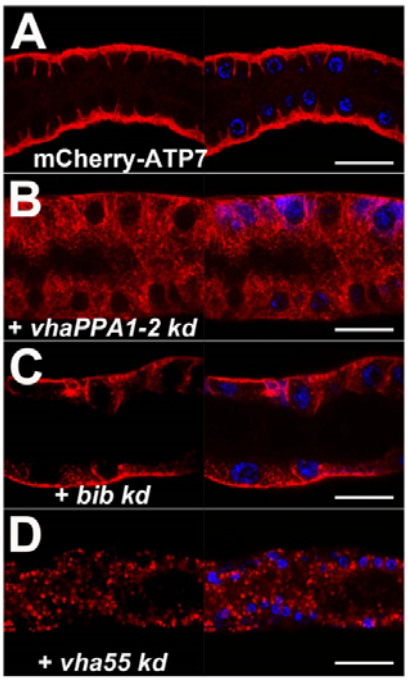

FIGURE 6

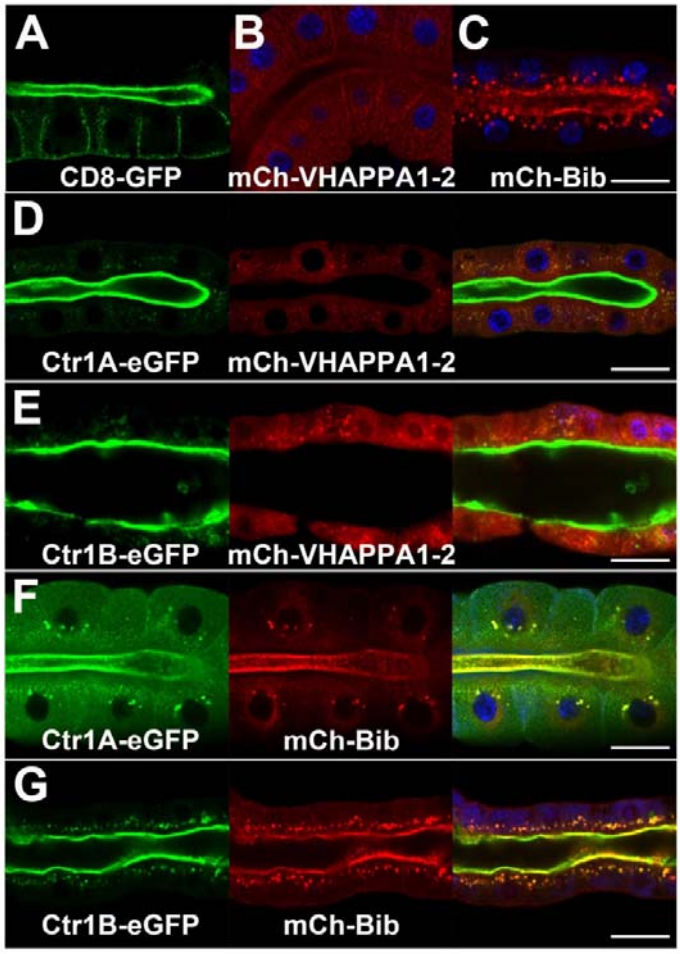

FIGURE 7

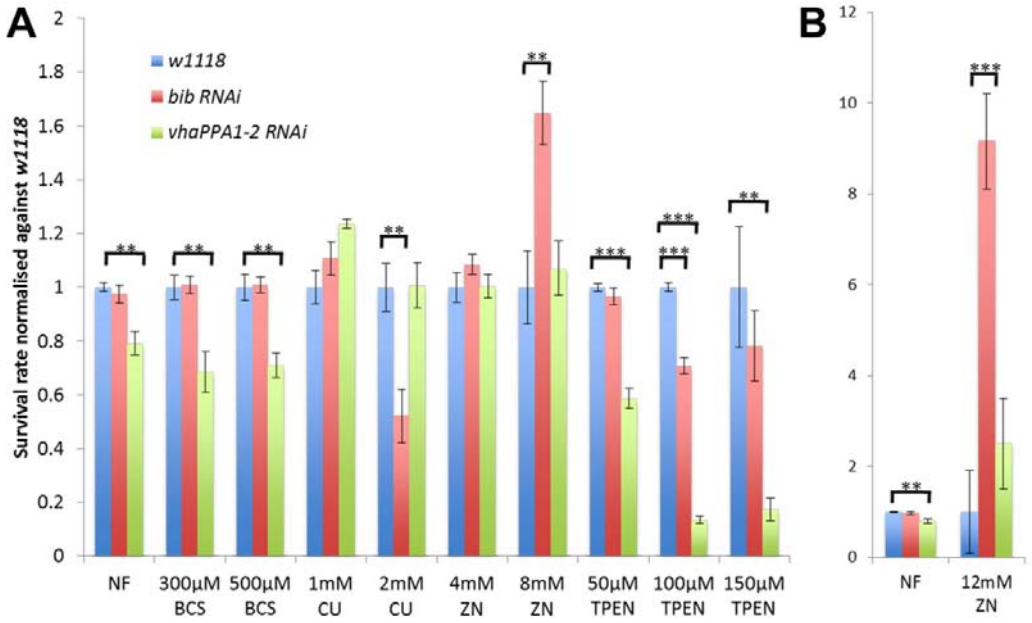

WANG ET AL 2014: SUPPLEMENTARY MATERIAL

Figure S1. Ectopic expression of *Ctr1A* or *Ctr1B* fails to rescue the hypo-pigmentation caused by knockdown of *vhaPPA1-2* or *bib*. All flies have *Pnr-Gal4*. kd = knockdown, oe = over-expression. A) *Pnr-Gal4>UAS-vhaPPA1-2*^{RNAi}*; UAS-Ctr1A*^{flag} fly with mild hypo-pigmentation still seen in the thorax and abdomen. B) *Pnr-Gal4>UAS-bib*^{RNAi}*; UAS-Ctr1A*^{flag} fly with moderate hypo-pigmentation still seen in the thorax and abdomen. C) *Pnr-Gal4>UAS-vhaPPA1-2*^{RNAi}*; UAS-Ctr1B*^{flag} fly with stripes of mild hypo-pigmentation still seen on the shoulders. D) *Pnr-Gal4>UAS-bib*^{RNAi}*; UAS-Ctr1B*^{flag} fly with moderate hypo-pigmentation still seen in the thorax and abdomen. Scale bar = 200 μm